

the first excited states of Ni^{58} and Ni^{60} ,⁵ and give negative parity for the anomalous state. The ambiguity in what value of the radius to use prevents a unique deduction of the spin of the state from the inelastic-scattering angular distribution.⁴ On the other hand, the angular correlation results can be interpreted as showing that the "anomalous state" is 3^- and decays to the first excited 2^+ state through the emission of electric dipole radiation^{4,6}. The results of a Born approximation calculation for the angular correlation are also illustrated in Fig. 3 for the two assumptions of electric dipole radiation from either a 1^- or 3^- state. By virtue of the fact that the gamma-ray spectrum shows transition directly from the anomalous level to the first and the relatively large number of levels⁷ between 1.5 and 4 Mev in both nuclei, it would seem unlikely that the state had any spin higher than 3^- .

A possible interpretation of this level is that it is a collective octupole oscillation.^{4,8} On the basis of a classical hydrodynamic approach to nuclear structure Bohr and Mottelson estimate the energy of the lowest octupole surface oscillation to be in the range of 4 to 7 Mev.⁹ However, further data relative to the transition probabilities will be necessary to establish this collective nature.⁸ Goodman¹⁰ has emphasized the single-particle explanation of the "anomalous levels." While accounting for a level in the inelastic particle spectrum at about 4-Mev excitation, he

makes no definite prediction as to its spin.

The authors would like to thank Professor M. Deutsch for his assistance and a number of valuable comments.

[†]This work is supported in part by funds provided by the U. S. Atomic Energy Commission, the Office of Naval Research, and the Air Force Office of Scientific Research.

[‡]On leave from Centre d'Etudes Nucléaires de Saclay, Gif-sur-Yvette, Seine et Oise, France.

¹B. L. Cohen and A. G. Rubin, *Phys. Rev.* **111**, 1568 (1958).

²J. L. Yntema and B. Zeidman, *Phys. Rev.* **114**, 815 (1959).

³D. R. Sweetman and N. S. Wall, *Comptes Rendus à Congrès International de Physique Nucléaire* (Dunod, Paris, 1958), p. 547.

⁴J. S. Blair (to be published); see also Yntema, Zeidman, and Raz (to be published).

⁵Strominger, Hollander, and Seaborg, *Revs. Modern Phys.* **30**, 585 (1958).

⁶G. R. Satchler, *Proc. Phys. Soc. (London)* **A68** 1037 (1958); C. A. Levinson and M. K. Banerjee, *Ann. Phys.* **2**, 499 (1957). The expression given in these references has been corrected by a phase factor and has been normalized to the experimental data.

⁷C. H. Paris and W. W. Buechner, *Comptes Rendus à Congrès International de Physique Nucléaire* (Dunod, Paris, 1958), p. 515.

⁸A. M. Lane and E. D. Pendelbury (to be published).

⁹A. Bohr and B. R. Mottelson, *Kgl. Danske Videnskab. Selskab, Mat.-fys. Medd.* **27**, No. 16 (1953).

¹⁰C. D. Goodman, *Phys. Rev. Letters* **3**, 230 (1959).

EXPERIMENTAL EVIDENCE FOR D WAVES IN π^-p SCATTERING AT 370 AND 427 Mev*

Lester K. Goodwin, Robert W. Kenney, and Victor Perez-Mendez
Lawrence Radiation Laboratory, University of California, Berkeley, California
(Received November 5, 1959)

The differential elastic scattering of pions on protons furnishes information on the magnitude of the various partial waves included in the interaction. Precise measurements of this process up to 333 Mev^{1,2} have been interpreted in terms of S and P waves and their six associated charge-independent phase shifts. No D or higher waves were necessary to give a statistically significant fit to the data. In this Letter, we report our values of the elastic-scattering cross section for negative pions on protons at 370 ± 9 and 427 ± 10 Mev (lab energies).

The experimental setup is shown in Fig. 1. The pion beam from an internal Be target in the

184-in. cyclotron was deflected out of the machine by its magnetic fringing field. The beam was then momentum-analyzed and focused by the wedge and quadrupole magnets shown. The intensity of the 2-in. diam beam was greater than 15 000 negative pions per second. The beam energy and its muon and electron contaminations were determined from ranges in copper.

The pion beam was scattered in a 4-in.-thick liquid-hydrogen target. The elastically scattered pions were detected by a three-scintillator counter telescope which discriminated against recoil protons and inelastic pions on the basis of range in the copper absorbers placed between

the first and last scintillators of the telescope. A different thickness of copper absorber was used for each energy of the elastically scattered pions. This energy was a unique function of the angle of scattering and was calculated from the kinematics of the two-body final state. The efficiency of the telescope was measured as a function of pion energy, with essentially the same pion beam setup shown in Fig. 1. Beam energy and contamination were determined from range curves.

The main corrections to the data are for Coulomb scattering, finite target and telescope size, and π^0 photons from charge-exchange scattering.³ The results of the experiment are shown in Fig. 2. Also shown is the differential cross section at zero degrees. The imaginary part of the forward-scattering amplitude was obtained from total cross-section data,^{1,4} and the real part was obtained from dispersion theory.⁵ Because of the relatively small contribution to the cross section of the real part compared to the imaginary part at these energies, even a 100% error in the real part does not significantly affect the cross-section magnitude or its error. Thus the zero-degree differential cross sections shown depend effectively only upon the experimentally determined total cross sections.

The data were fitted to a power series in $\cos\theta^*$, where θ^* is the center-of-mass scattering angle,

$$d\sigma/d\Omega^* = \sum_{k=0}^n A_k (\cos\theta^*)^k,$$

for various values of n . Three of the least-squares fits made at each energy are shown in Fig. 2. The dashed curve represents the fit to the points, excluding the calculated zero-degree

point and using only S - and P -wave contributions ($n=2$). The dot-dash curve represents the fit to the same points obtained for a value of n that was

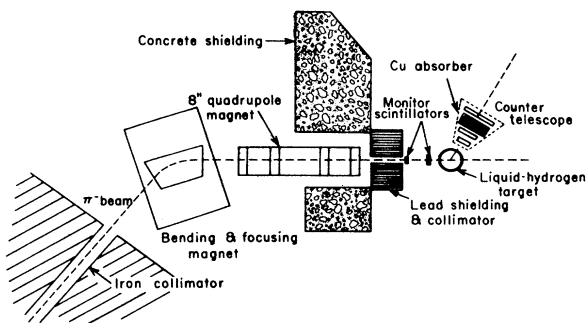


FIG. 1. Experimental arrangement (not to scale).

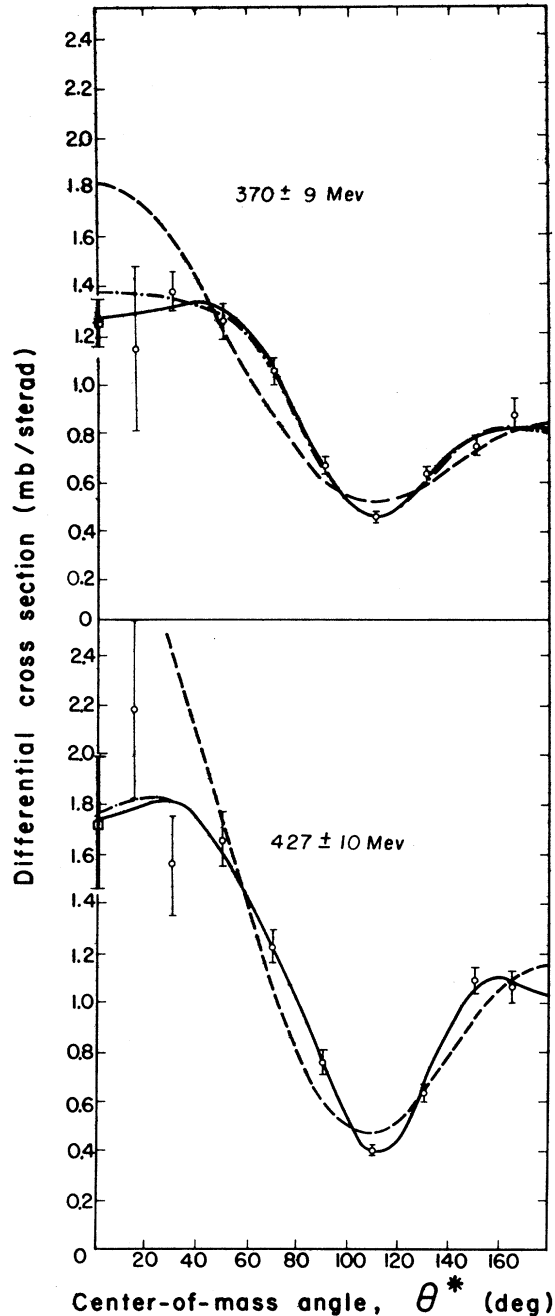


FIG. 2. Differential cross sections for $\pi^- - p$ elastic scattering. The square points on the ordinates represent dispersion-relation predictions. The solid curve represents the best least-squares fit obtained including the zero-degree point. The dot-dash curve represents the best fit obtained excluding the zero-degree point. The dashed curve represents the fit obtained excluding the zero-degree point and using only S and P waves.

Table I. Least-squares-fit parameters, A_k , in millibarns/steradian, for the most probable values of n , for which p is the probability that χ^2 for a random sample would exceed the value found.

Energy (Mev)	n	Zero-deg point	A_0	A_1	A_2	A_3	A_4	A_5	A_6	p (%)
370 \pm 9	5	included	0.65 ± 0.03	1.02 ± 0.10	0.97 ± 0.18	-1.43 ± 0.40	-0.57 ± 0.19	0.65 ± 0.35		44
370 \pm 9	5	excluded	0.66 ± 0.03	1.03 ± 0.11	0.89 ± 0.25	-1.56 ± 0.51	-0.45 ± 0.32	0.81 ± 0.52		28
427 \pm 10	6	included	0.77 ± 0.04	1.46 ± 0.16	0.19 ± 0.56	-2.15 ± 0.73	2.50 ± 1.68	1.04 ± 0.65	-2.07 ± 1.26	34
427 \pm 10	6	excluded	0.77 ± 0.05	1.47 ± 0.21	0.20 ± 0.70	-2.19 ± 1.05	2.43 ± 2.20	1.10 ± 1.06	-1.99 ± 1.78	19

chosen on the basis of a χ^2 test to have its most probable value. The solid curve represents the fit obtained for the most probable value of n when the zero-degree point is included. The values of the best-fit parameters, A_k , are given in Table I. The table also gives the probabilities, p , that χ^2 for a random sample would exceed the value found.

The probabilities that the data are consistent with the fits based on S and P waves alone is less than 1%. Thus the inclusion of D waves is necessary to obtain a reasonable fit to the data. In fact, the most probable values of n obtained include an F -wave interference term ($n=5$) at 370 Mev and an F -wave term ($n=6$) at 427 Mev. The conclusion is that D waves are present, and that F waves may be present, especially at 427 Mev.

The total elastic cross sections, obtained from integrating the solid-line fits, are 10.8 ± 0.2 mb at 370 Mev and 13.00 ± 0.34 mb at 427 Mev. The zero-degree differential cross sections obtained by extrapolating the dot-dash curves to 0° are 1.38 ± 0.23 mb/sterad at 370 Mev and 1.78 ± 0.55

mb/sterad at 427 Mev. Within statistics these values agree with those predicted from dispersion relations.

We should like to acknowledge the continued interest and support of Professor A. C. Helmholtz, and to thank Dr. Walton A. Perkins and Mr. James Vale and the cyclotron crew for their assistance and cooperation during the course of the experiment.

* Work done under the auspices of the U. S. Atomic Energy Commission.

¹H. A. Bethe and F. de Hoffmann, Mesons and Fields II (Row, Peterson, and Company, White Plains, 1955).

²V. G. Zinov and S. M. Korenchenko, Zhur. Eksptl. i Teoret. Fiz. 34, 301 (1958) [translation: Soviet Phys. JETP 34, 210 (1958)].

³Caris, Kenney, Knapp, Perez-Mendez, and Perkins, University of California Radiation Laboratory Report, UCRL-8904, September, 1959 (unpublished).

⁴Mukhin, Ozrov, and Pontecorvo, Zhur. Eksptl. i Teoret. Fiz. 31, 371 (1956) [translation: Soviet Phys. JETP 4, 237 (1957)].

⁵H. J. Schnitzer and G. Salzman, Atomic Energy Commission Report, NYO-2265, August, 1958 (unpublished).